An exploratory study of loading and morphometric factors associated with specific failure modes in fatigue testing of lumbar motion segments

Sean Gallagher [a,*], William S. Marras [b], Alan S. Litsky [c], Deborah Burr [d]

[a] National Institute for Occupational Safety and Health, Mining Injury Prevention Branch, P.O. Box 18070, Pittsburgh, PA 152360070, USA
[b] Biodynamics Laboratory, The Ohio State University, Columbus, OH 43210, USA
[c] Orthopaedic BioMaterials Laboratory, The Ohio State University, Columbus, OH 43210, USA
[d] Department of Health Services, Research Management, and Policy, University of Florida, Gainesville, FL 32611, USA

Abstract

Background. There is currently little information regarding factors associated with specific modes of motion segment failure using a fatigue failure model.

Methods. Thirty-six human lumbar motion segments were fatigue tested using spinal compressive and shear loads that simulated lifting a 9 kg weight in three torso flexion angles (0°, 22.5°, and 45°). Twenty-five segments failed via fatigue prior to the 10,000 cycle maximum. These specimens were visually inspected and dissected so that the mode(s) of failure could be determined. Failure modes included endplate fractures (classified into nine varieties), vertebral body fractures, and/or zygapophysial joint disruption. Logistic regression analyses were performed to determine whether certain morphometric variables, amount of motion segment flexion, disk degeneration scores, and/or loading characteristics were associated with the occurrence of specific failure modes.

Findings. Results indicated that stellate endplate fractures were associated with increased posterior shear forces ($P < 0.05$) and less degenerated discs ($P < 0.01$). Fractures running laterally across the endplate were associated with motion segments having larger volumes ($P < 0.01$). Endplate depression was more common in smaller specimens ($P < 0.01$), as well as those experiencing increased posterior shear force ($P < 0.05$). Zygapophysial joint damage was more likely to occur in a neutral posture ($P < 0.01$).

Interpretation. These results suggest that prediction of failure modes (e.g., specific endplate fracture patterns) may be possible (at least for older specimens) given knowledge of the spinal loads along with certain characteristics of the lumbar spine.
Published by Elsevier Ltd.

Keywords: Lumbar spine; Endplate fractures; Zygapophysial joints; Morphometry; Disk degeneration; Motion segments; Aging

1. Introduction

As with any material, spinal tissues will fail when an applied load exceeds the tissue tolerance (Litsky and Spector, 1999). Failure may be the result of a single application of a large load (exceeding the ultimate strength of the material) or may result from repeated application of a sub-maximal load via fatigue failure (McGill, 1996). Given the repetitive nature of spine loading in many occupational (as well as non-occupational) settings (Brinckmann et al., 1988; Marras et al., 1993), the latter scenario would seem orthopaedically significant. Nonetheless, fatigue failure of lumbar tissues has received relatively little attention in the literature.

---

* Corresponding author.
E-mail address: sgallagher@cdc.gov (S. Gallagher).

The magnitude and distribution of loads on structural components of the lumbar spine vary considerably based upon numerous factors, and these will influence the structures and/or patterns of failure observed. Among the factors influencing load magnitude and distribution are the posture adopted by a motion segment (White and Panjabi, 1978), the amount and distribution of bone mineral content (Hayes, 1986; Rockoff et al., 1969), the size of the vertebral bodies and discs (Jager and Luttmann, 1991; White and Panjabi, 1978), the degree of disc degeneration (Kulak et al., 1976), and the magnitude of the compressive and shear forces imposed upon the spine (Jager and Luttmann, 1991; Begemann et al., 1994). As an example, zygapophysial joints are thought to bear approximately 15–20% of the compressive load experienced by a motion segment in a neutral position (Adams and Hutton, 1980; Adams and Hutton, 1983). However, when the spine is flexed, this loading path may be reduced (White and Panjabi, 1978) and the compressive load may be increasingly borne by the inter-body joint (the joint comprised of two vertebral bodies and their adjoining disk). The increased burden experienced by the inter-body joint would amplify the stress imposed on the vertebral endplates and discs, which will experience additional strain and increased potential for failure.

The vertebral endplate appears to be the tissue most likely to experience initial failure in tests of both ultimate compressive strength and fatigue failure (Brown et al., 1957; Perey, 1957). A variety of endplate fracture patterns have been observed and Brinckmann et al. (1988) developed a useful classification system for various modes of endplate damage. Vertebral body fractures and disruption of the zygapophysial joints are also observed in compressive loading tests; however, failure of the intervertebral discs are less frequent (Bogduk, 1997). Discs may fail when compressed in flexion (Adams and Hutton, 1982) when compressed in flexion combined with an axial twist (Gordon et al., 1991), or as the result of a cascade initiated by endplate failure (Adams et al., 2000). Research using porcine models has suggested that disc herniation also can be caused by repeated flexion and extension under moderate compressive loads (Callaghan and McGill, 2001).

Evaluating factors associated with specific failure modes exhibited by lumbar motion segments may assist in developing improved models of the manner of tissue failure and may ultimately assist in our understanding of the etiology of low back pain. Accordingly, the current exploratory study was performed to determine factors associated with specific failure modes in a study examining fatigue failure of lumbar motion segments exposed to loadings estimated to occur when lifting in various torso flexion postures.

2. Methods

Twelve fresh, frozen lumbar spines, with a mean age of 81 years (SD 8) were obtained from the Anatomical Gift Program at Wright State University. Specimens were excised within 24 h after death from subjects having no history of spinal disease or prolonged bed rest prior to death. Specimens were thawed at room temperature prior to dissection and testing. Intact lumbar spines were dissected into three separate motion segments: L1–L2, L3–L4, and L5–S1.

Anterior–posterior (A–P) and left lateral (LLAT) radiographs of each intact motion segment were obtained and served to detect the presence of existing defects in individual motion segments and were used to make various morphometric measurements of intact motion segments via measurement tools provided in eFilm xray viewing software (Merge eFilm, Milwaukee, WI, USA). Estimates of the volume of the inter-body joint (i.e., two vertebral bodies and intervening disc, not including posterior elements) of each motion segment were calculated on the basis of selected dimensions of the vertebral bodies and discs.

Vertebral bodies were potted in trays containing polymethylmethacrylate (PMMA), the orientation to the vertical of each motion segment being confirmed by endplate measurements obtained via multiple radiographs during the fixation process. Once specimens were properly oriented according to the torso flexion posture being simulated, they were placed in test fixtures attached to a servohydraulic test frame [Bionix 858, MTS Systems, Eden Prairie, MN, USA]. The test fixtures were situated within an environmental chamber whose temperature was kept at approximately 37 °C. Moisture was introduced into the chamber to maintain a humid environment.

Care was exercised to reproduce compressive and shear loads and spinal postures adopted when lifting a 9 kg box in three trunk flexion angles: 0° (neutral posture, as if standing erect), 22.5° (partial flexion), and 45° (full flexion). A dynamic electromyographically-assisted biomechanical model was used to develop appropriate compressive and shear loads and rates of loading at each torso flexion angle and lumbar level (Granata and Marras, 1995; Marras and Granata, 1997; Marras et al., 2001; Jorgensen et al., 2001). Details of the loadings used can be obtained in Table 1. Motion segments within each spine were randomly assigned to torso flexion angles. Motion segments were creep loaded for 15 min and then cyclically loaded (using load control) at 0.33 Hz until failure or the maximum number of cycles (10,000) was completed. Failure was defined as a displacement of 10 mm after termination of the period of creep loading. Twenty-five of the 36 motion segments failed via fatigue before the maximum number of cycles were completed. Those that lasted were subjected

Table 1
Endplate fracture patterns and zygapophysial joint damage experience for motion segments failing via fatigue in simulated lifting of 9 kg load in different torso flexion angles

Spine ID	Motion segment	Torso flexion	Absolute motion segment flexion	Motion segment flexion	Compression (N)	Shear (N)	Load rate (N/s)	Disk grade	Inferior EP (Sup. Vertebra)	Superior EP (Inf. Vertebra)	Zygapophysial joint damage
M11	L1–L2	22.5	1	1	2157	−1052	2100	3	1,6	4	*
	L3–L4	45	−2	6	2700	−1622	4800	3		9	
M8	L1–L2	45	3	3	2878	−1281	4800	2	6	6	
M1	L1–L2	0	0	0	1178	−549	700	3	2		*
	L3–L4	22.5	−5	3	2255	−821	2100	2	2,1		*
	L5–S1	45	−14	6	3127	−541	4800	2	2,6		
F9	L1–L2	45	3	3	2878	−1281	4800	3	4,5	5	
	L5–S1	0	−20	0	1196	507	700	3		6	*
M7	L1–L2	22.5	1	1	2157	−1052	2100	3	6,5	6	
	L5–S1	45	−14	6	3127	−541	4800	4	6		*
F6	L3–L4	45	−2	6	2700	−1622	4800	2	1		*
F17	L1–L2	22.5	1	1	2157	−1052	2100	3	1	6	
	L3–L4	45	−2	6	2700	−1622	4800	2	6	1,6	*
	L5–S1	0	−20	0	1196	507	700	2		6	*
M10	L1–L2	45	3	3	2878	−1281	4800	2	1,4	8	
	L5–S1	22.5	−17	3	2386	251	2100	3		4,5,6	*
F13	L1–L2	0	0	0	1178	−549	700	3	6		*
	L1–L4	22.5	−5	3	2255	−821	2100	2	1,6	6	
	L5–S1	45	−14	6	3127	−541	4800	2	1	1	
M16	L1–L2	45	3	3	2878	−1281	4800	2	1		
	L3–L4	22.5	−5	3	2255	−821	2100	1	1,5		*
M12	L1–L2	22.5	1	1	2157	−1052	2100	3	2,7		
	L5–S1	45	−14	6	3127	−541	4800	3	2,5		
M14	L3–L4	45	−2	6	2255	−821	4800	2	1	6,5	
	L5–S1	22.5	−17	3	2386	251	2100	3	6,5	6,5	

Disc degeneration grades are given per Galante (1967). Refer to Fig. 1 for classification of endplate fractures.

to a test of ultimate compressive strength. The latter were not included in the present analysis due to the extensive damage associated with this mode of testing.

Upon completion of the mechanical testing, specimens were removed from the loading jigs and taken to the radiology clinic to evaluate damage using a lateral radiograph. These radiographs were read to evaluate the post-test status of the endplates, vertebral bodies, trabeculae, intervertebral discs, and posterior elements. Visual inspection of failed specimens was performed to evaluate external evidence of failure, particularly facet disruption and/or external evidence of fracture to the vertebral bodies. The PMMA-specimen interface was scrutinized to ensure that failure did not occur at this interface. Failed specimens were dissected through the mid-plane of the intervertebral disc, digitally photographed and a Galante disc degeneration score assigned to each of the discs. The endplates were then exposed and assessed for damage.

The Brinckmann et al. (1988) classification scheme did not fully characterize the nature of the endplate fractures observed in this investigation, and a modified version of the classification system was developed. This new classification system, illustrated in Fig. 1, includes many of the original Brinckmann et al. (1988) classifications, but adds some additional classifications of endplate damage (ring fractures, lateral fractures and A–P fractures) observed in the current study. Two of the Brinckmann et al. (1988) classifications were omitted in this new system. These included the "transverse" fracture, which appears to represent a fracture of the vertebral body rather than the endplate, and the "Y" fracture, observed only twice in the Brinckmann et al. (1988) original experiment, and not observed in the present study.

2.1. Data analysis

A series of stepwise logistic regression analyses were performed to evaluate the association between various motion segment and load characteristics and failure modes observed in post-test examination and dissection.
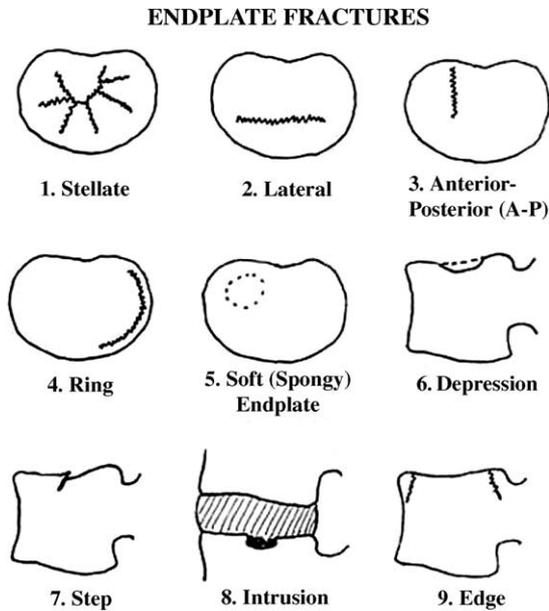
ENDPLATE FRACTURES

Fig. 1. Endplate fracture classification scheme modified from Brinck-mann et al. (1988).

The analysis was performed on the 25 motion segments failing via fatigue failure; thus, results represent a conditional probability based on failure by this mode. Independent variables included motion segment characteristics including Galante disc degeneration grade (Galante, 1967), estimated volume of the inter-body joint, the degree of flexion from a neutral position, and weight (g) of the motion segment. Loading characteristics, comprising the balance of independent variables, included compressive and shear forces experienced by the motion segment and the rate at which specimens were loaded. Each failure mode (the nine endplate fracture patterns, fractures of superior and inferior vertebral bodies, and zygapophysial joint disruption) was treated as the dependent variable in separate stepwise logistic regressions using the independent variables listed above. As an exploratory analysis, multiplicity corrections were not applied in the data analyses (Bender and Lange, 2001). Specifically, a comparisonwise Type I error rate alpha level of 0.05 was employed.

3. Results

Table 1 provides a summary of motion segment characteristics along with endplate fractures patterns and occurrence of zygapophysial joint damage observed for all motion segments failing via fatigue in the experiment. Table 2 provides results of the logistic regression analyses relating specific failure modalities to the various independent factors manipulated in the study.

3.1. Endplate fracture patterns

Several endplate fracture patterns were associated with specific changes in the independent variables under study (Table 2). Stellate endplate fractures were associated with less degenerated discs ($P < 0.005$) and increased shear forces on the motion segment ($P < 0.05$). Fissures running laterally across the endplate were observed to occur more frequently with motion segments of larger volume ($P < 0.005$). Depression of the endplate was a more frequent finding in specimens having smaller volume ($P < 0.01$) and experiencing higher levels of shear force ($P < 0.05$).

3.2. Zygapophysial joints

As can be seen in Table 2, zygapophysial joint damage was significantly associated with the degree of torso flexion ($P < 0.01$). Examination of Table 1 shows that zygapophysial damage was present in 100% of the specimens failing via fatigue in the simulated neutral trunk posture. Damage was observed in three of nine (33%) specimens in the 22.5° torso flexion condition, and three out of twelve specimens (25%) exposed to the 45° torso flexion condition exhibited damage. Thus, the likelihood of damage to the facets was greatest in the neutral posture, and was diminished as greater flexion of the motion segment was assumed.

4. Discussion

This investigation is the first, to the authors' knowledge, to uncover statistical associations between both

Table 2
Summary of significant logistic regression results relating variables to specific failure modes (*Note*: MS = motion segment, AP = anterior–posterior, EP = endplate)

Failure mode	Significant variable associations	*P*	Nature of association
Stellate EP fracture	Galante grade	0.006	↓Galante: ↑Stellate fracture
	AP shear	0.019	↑Post. Shear: ↑Stellate fracture
Lateral EP fracture	MS volume	0.003	↑Volume: ↑Lateral fracture
EP depression	MS volume	0.006	↓Volume: ↑EP depression
	AP shear	0.015	↑Post. Shear: ↑EP depression
Facet damage	Torso flexion	0.009	↓Flexion: ↑Facet damage

motion segment loading characteristics and the occurrence of specific endplate fracture patterns and zygapophysial joint damage. Factors found to influence endplate fracture patterns include the degree of disc degeneration of the specimen, the size of the specimen, and the amount of shear force experienced. Zygapophysial joint damage was influenced by the posture adopted by motion segments failing via fatigue.

Several of the associations uncovered in this investigation appear readily interpretable. For example, stellate endplate fractures were found to be associated with greater shear force exposure and less degenerated discs. Bone is an anisotropic material and is more susceptible to damage when exposed to shear force (Litsky and Spector, 1999). It may be that exposure to higher shear forces undermines the support of the endplate via damage to the underlying trabecular arcades. The more centralized pressure distribution on the endplate associated with less degenerated discs (Bogduk, 1997), combined with the reduced support of the endplate resulting from trabecular shear damage, and may result in a stellate fracture pattern where a focal area of fracturing is observed centrally in the endplate with cracks radiating to the periphery.

Motion segments having smaller volumes and higher shear forces were associated with increased incidence of endplate depression. It should be pointed out that the compressive and shear loads were identical no matter the size of the specimen. Thus, smaller specimens would experience a more concentrated distribution of stress that may increase the likelihood of endplate depression. Larger specimens would have the same force distributed over a larger area, which may decrease the propensity to centrally depress the endplate. Increased shear force may again undermine the support of the endplate leading to increased incidence of depressed endplates.

This study involved the modification of an endplate fracture classification structure proposed by Brinckmann et al. (1988). Results clearly support the use of an endplate damage classification system, as different endplate damage classifications were observed to have significant associations with certain motion segment and loading characteristics. Two of the original Brinckmann et al. (1988) classifications were found to have significant associations with such characteristics (i.e., stellate fractures and endplate depressions). However, one of the new endplate fracture classifications (a fracture running laterally across the endplate) was also found to exhibit a significant association with specimen morphometry. This result would seem to support the suggested modifications of the original classification system. As research in this area continues, it may be possible to develop further refinements to endplate damage classifications. Such a process may continue to improve our understanding of the factors associated with the manner of endplate failure.

Studies have indicated that compression of a motion segment in a neutral posture may lead to damage to the zygapophysial joints, a finding supported by the current analysis. When subject to severe or repeated compression in this position, the superior facets impact the lamina below, pushing the facets backwards, ultimately resulting in joint disruption. In a flexed position, these joints assume a progressively smaller load-bearing responsibility (White and Panjabi, 1978) and failure appears to occur primarily in the inter-body joint with a progressively lower likelihood of facet involvement.

It is remarkable that, even given a relatively small sample of motion segments, several significant associations were uncovered relating morphologic and loading variables to specific failure patterns. Results suggest that by knowing certain characteristics of the spine and the manner of loading, one may be able to predict which structures may be at increased risk of failure and perhaps even predict what pattern of that failure might result. It is noteworthy that most of the significant independent variables used in this analysis (degree of disc degeneration, size of the specimen, shear forces) can be measured or estimated using in vivo techniques. The current results certainly suggest the possibility that such measures could be evaluated in vivo and may allow prediction as to the likely structure of failure in the lumbar spine and even the likely failure pattern. However, one should bear in mind that the results of the current study are exploratory in nature and will need to be tested in further confirmatory studies. Clearly, much additional research will be necessary to confirm the present results and potentially identify additional associations.

A complete assessment of the experimental results described above requires the consideration of certain limitations. The first of these deals with the age of the cadaveric cohort studied. Unfortunately, the vendor used to obtain the lumbar spines used in this study was unable to provide specimens under the age of 65. As a result, it becomes difficult to generalize the results of this study to the younger, working age population that is the intended beneficiary of the research. Younger spines would be expected to have increased bone mineral content and density than the older spines tested in this study, and failure patterns may differ as a result. Efforts are currently underway to obtain a sample of spines more representative of a working age population to continue this research. It may be noted that specimens were loaded in compression and shear with motion segments preset at the desired Cobb angles, instead of generating the motion segment flexion via an anterior offset in the application of force. Analysis of free body diagrams demonstrate that whether the motion segment is preset in flexion or flexed to the same degree by applying a bending moment, application of equivalent compressive and shear forces will result in equivalent reaction forces being experienced by the specimen. The current loading

situation did not generate a "rocking" motion of the motion segment as an offset load would; however, the authors opted for the more precise control offered by loading the specimen at the desired flexion angle.

The lumbar spine is one part of a complex physiologic system and isolation of the spine (or its motion segments) necessarily alters the loading situation compared to the in vivo environment. Studies performed on animals have suggested a possible change in mechanical behavior of various tissues after death (Keller et al., 1990); however, the differences attributed to death in this experiment were not much larger than trial to trial variability on the live animal (Adams and Dolan, 1995). However, the process of dissecting out motion segments necessitates a weakening of ligaments of the spine that have fibers spanning multiple vertebrae (Adams, 1995). There are also obvious differences between the manner in which spine segments are loaded with functioning muscles and tendon attachments as opposed to a specimen potted in polymethylmethacrylate and *loaded* in a test frame. Nonetheless, the methods of *in vitro* testing employed here remain one of our best methods to improve our understanding of the mechanical responses of lumbar tissue.

While radiographs were obtained and abnormal external findings were noted during dissection, it is possible that pre-existing damage, particularly to the endplates, may have been present prior to testing but not detected. It is extremely difficult to detect endplate fractures via regular radiographs or other imaging techniques (White and Panjabi, 1978). Thus, it is conceivable that some of the damage reported in the posttest evaluations was pre-existing, and not the result of the stresses imposed during testing. Certainly the tests could have also exacerbated pre-existing damage in the specimens, causing failure to occur more quickly than would have occurred to an intact specimen. However, the statistical results obtained in this analysis indicate that the associations uncovered are beyond random chance occurrences. Thus, unless we believe that the randomization procedure was extremely unlucky, we must conclude that the failure modes observed are influenced by the factors identified above.

5. Conclusions

On the basis of the current investigation, the following conclusions are drawn:

1. Endplate fractures patterns and zygapophysial joint damage in this older cohort of lumbar spines were significantly associated with variables such as motion segment morphometry, degree of flexion, disk degeneration, and the nature of the applied loads in fatigue failure.

2. Stellate endplate fractures were associated with increased shear exposure and less degenerated disks. Lateral endplate fractures were found to be associated with specimens with larger inter-body joint volume. Endplate depression was associated with lower exposure to shear and smaller specimens.

3. Zygapophysial joint damage was more likely in the neutral posture condition, and progressively less likely with increasing flexion in specimens failing via fatigue.

4. A modified endplate damage classification system is suggested, and data from this study provide support for the modified system.

5. Results suggest that prediction of specific failure modes for older lumbar motion segments may be possible given knowledge of the specimen size, disk degeneration status, degree of flexion and spine loading characteristics.

References

Adams, M.A., 1995. Spine update: mechanical testing of the spine: an appraisal of methodology, results, and conclusions. Spine 20, 2151–2156.

Adams, M.A., Dolan, P., 1995. Recent advances in lumbar spinal mechanics and their clinical significance. Clin. Biomech. 10, 3–19.

Adams, M.A., Hutton, W.C., 1980. The effect of posture on the role of the apophyseal joints in resisting compressive force. J. Bone Joint Surg. 62B, 358–362.

Adams, M.A., Hutton, W.C., 1982. Prolapsed intervertebral disc: a hyperflexion injury. Spine 7, 184–190.

Adams, M.A., Hutton, W.C., 1983. The mechanical function of the lumbar apophyseal joints. Spine 8, 326–330.

Adams, M.A., Freeman, B., Morrison, H.P., Nelson, I.W., Dolan, P., 2000. Mechanical initiation of intervertebral disc degeneration. Spine 25, 1625–1636.

Begemann, P.C., Visarius, H., Nolte, L.-P., Prasad, P., 1994. Visocelastic shear responses of the cadaver and Hybrid III lumbar spine. Wayne State University, Detroit, Mich./Mueller Institute for Biomechanics/Ford Motor Company, Dearborn, Mich. 1994. 14p. Stapp Car Crash Conference. Thirty-eighth. Proceedings. Warrendale, SAE, Nov 1994, pp. 1–14.

Bender, R., Lange, S., 2001. Adjusting for multiple testing—when and how? J. Clin. Epidemiol. 54, 343–349.

Bogduk, N., 1997. Clinical Anatomy of the Lumbar Spine and Sacrum, Third Ed Churchill Livingstone, New York, NY, 261.

Brinckmann, P., Biggemann, M., Helweg, D., 1988. Fatigue fracture of human lumbar vertebrae. Clin. Biomech. 3 (Suppl. 1), S1–S23.

Brown, T., Hansen, R.J., Yorra, A.J., 1957. Some mechanical tests on the lumbosacral spine with particular reference to the intervertebral disc. J. Bone Joint Surg. 39A, 1135–1164.

Callaghan, J.P., McGill, S.M., 2001. Intervertebral disc herniation: studies on a porcine model exposed to highly repetitive flexion/extension motion with compressive force. Clin. Biomech. 16, 28–37.

Galante, J.O., 1967. Tensile properties of the human lumbar annulis fibrosus. Acta Orthopaed. Scand. Suppl. 100, 1–91.

Gordon, S.J., Yang, K.H., Mayer, P.J., Mace, A.H., Kish, V.C., Radin, E.L., 1991. Mechanisms of disc rupture: a preliminary report. Spine 16, 450–456.

Granata, K.P., Marras, W.S., 1995. An EMG-assisted model of trunk loading during free-dynamic lifting. J. Biomech. 28, 1309–1317.

Hayes, W.C., 1986. Bone mechanics: from tissue mechanical properties to an assessment of structural behavior. In: Scmid-Schonbein, W.W., Woo, S.L.-Y., Zweifach, B.W. (Eds.), Chapter in Frontiers in Biomechanics. Springer-Verlag, New York, pp. 196–209.

Jager, M., Luttmann, A., 1991. Compressive strength of lumbar spine elements related to age, gender, and other influences. Electromyographical Kinesiology, Proceedings of the 9th Congress of the International Society of Electrophysiological Kinesiology, pp. 291–294.

Jorgensen, M.J., Marras, W.S., Granata, K.P., Wiand, J.W., 2001. MRI-derived moment-arms of the female and male spine loading muscles. Clin. Biomech. 16, 182–193.

Keller, T.S., Holm, S.H., Hansson, T.H., Spengler, D.M., 1990. The dependence of intervertebral disc mechanical properties on physiologic conditions. Spine 15, 751–761.

Kulak, R.F., Belytschko, T.B., Schultz, A.B., Galante, J.O., 1976. Non-linear behaviour of the human intervertebral disc under axial load. J. Biomech. 9, 377–386.

Litsky, A.S., Spector, M., 1999. Biomaterials, 2nd ed. In: Buckwalter, J.A., Einhorn, T.A., Simon, S.R. (Eds.), Chapter in Orthopaedic Basic Science American Academy of Orthopaedic Surgeons Press, Rosemont, IL.

Marras, W.S., Granata, K.P., 1997. The development of an EMG-assisted model to assess spine loading during whole-body free-dynamic lifting. J. Electromyography Kinesiol. 7, 259–268.

Marras, W.S., Lavender, S.A., Leurgans, S.E., Rajulu, S.L., Allread, W.G., Fathallah, F.A., Ferguson, S.A., 1993. The role of dynamic three-dimensional motion in occupationally-related low back disorders. The effects of workplace factors, trunk position, and trunk motion characteristics on risk of injury. Spine 18, 617–628.

Marras, W.S., Jorgensen, M.J., Granata, K.P., Wiand, B., 2001. Female and male trunk geometry: size and prediction of the spine loading trunk muscles derived from MRI. Clin. Biomech. 16, 38–46.

McGill, S.M., 1996. The biomechanics of low back injury: implications on current practice in industry and the clinic. J. Biomech. 30, 465–475.

Perey, O., 1957. Fracture of the vertebral end-plate in the lumbar spine. Acta Orthopaed. Scand. Suppl. 25, 1–101.

Rockoff, S., Sweet, E., Bleustein, J., 1969. The relative contribution of trabecular and cortical bone in the strength of the human lumbar vertebrae. Calicified Tissue Res. 3, 163–175.

White, A.A., Panjabi, M.M., 1978. Clinical Biomechanics of the Spine. JB Lippincott, Philadelphia.